Optics and Lasers in Engineering **8** (1988) 123–136

A Windowing Technique for the Automated Analysis of Holo-Interferograms

D. R. Matthys,[a] J. A. Gilbert,[b] T. D. Dudderar[c] and K. W. Koenig[a]

[a] Physics Department, Marquette University, Milwaukee WI 53233, USA, [b] Department of Mechanical Engineering, University of Alabama in Huntsville, Huntsville, Alabama 35899, USA and [c] AT&T Bell Laboratories, Murray Hill, New Jersey 07974, USA

(Received 22 January 1987; revised version received 24 August 1987; accepted 25 August 1987)

ABSTRACT

A systematic method for measuring surface deformations is described which includes the use of real-time holographic interferometry, the incorporation of a carrier fringe pattern to achieve fringe linearization, and the application of image digitization and automated computer analysis for rapid quantitative interpretation. In this method, regions of interest can be selected by the use of a windowing technique in which the operator specifies the desired subregion. The problem of correctly numbering fringes which originate or vanish at the boundary where the scanning begins is solved by an algorithm which ensures correct identification of the fringe orders. The output includes a perspective plot of the out-of-plane deformation field.

This method is demonstrated by its application to a measurement of the out-of-plane deformation of a hermetically sealed plastic housing loaded by internal pressurization.

INTRODUCTION

Although interferometry is sometimes said to be one of the most significant applications of holography, it has not yet found widespread practical application. The major factor inhibiting full exploitation of the technique is the difficulty of getting quantitative results from holographic interferograms. Indeed, by itself the interferogram does not even contain sufficient information to determine the direction or sign of the surface displacement component being measured. However,

Optics and Lasers in Engineering 0143-8166/88/$03·50

the real difficulty is that in practical cases the interference patterns obtained are frequently so complex that, even if the signs of the displacements were known, a skilled analyst could obtain quantitative results only with the expenditure of considerable time and effort. Therefore, if holo-interferometry is to be commonly used as a measurement tool, some method of simplifying the analysis of interferograms must be developed. This simplification can be attained through image processing and computer analysis.

Early efforts to use digital methods in the study of holo-interferograms were limited to linear fringe distributions.[1–3] Analysis of more complex displacements required the introduction of carrier fringes. This procedure was suggested by several investigators,[4–6] and has been used by the authors for semi-automatic analysis of deflection (out-of-plane displacement).[7]

This paper discusses the measurement of surface deflections induced by internal pressure variations on a hermetically sealed package used to house microelectronic components. The results obtained show that a high level of automation can be achieved by using a photoelectronic-numerical system for analysis of real-time holographic interferograms. At the same time, problems resulting from geometrical discontinuities on the surface or abrupt changes in reflectivity indicate a need for the development of more sophisticated numerical algorithms before arbitrary surfaces can be fully analyzed. However, even if a particularly complex surface cannot be studied as a whole, the use of a windowing technique allows subregions of interest to be selected and analyzed.

THEORY AND BACKGROUND

Most holo-interferometric fringe patterns obtained in practical applications are too complex to be readily amenable to automated analysis. However, a carrier fringe pattern may be used to achieve fringe linearization.[4–7] This technique involves superimposing a known linear phase shift on the phase changes caused by surface deformation to produce a monotonically changing phase distribution across the interferogram. In this way, the complex fringes of the original interferogram are reduced to 'nearly straight' fringes on which the deformation is superimposed as a modulation. Such fringes can easily be read in by a machine vision system. When the carrier fringes are later subtracted, the original information about the deformation is retrieved. In addition, the known phase characterisitcs of the carrier allow unambiguous determination of the sign of the displacement vector.

The use of single mode optical fibers for object and reference beam illumination greatly simplifies the required experimental set-up for conventional holographic and holo-interferometric applications.[8] When coupled with modern 'instant' holographic recording systems, optical fibers provide a powerful new tool for optical measurement.[9]

A holo-interferometric fringe pattern can be related to the deformation of the surface by the simple vector expression

$$n\lambda = \mathbf{g} \cdot \mathbf{d} \tag{1}$$

where n is the fringe order number, λ is the wavelength of the coherent light used to record and reconstruct the hologram, $\mathbf{g}$ is the sensitivity vector $(\mathbf{e}_2 - \mathbf{e}_1)$, where $\mathbf{e}_1$ and $\mathbf{e}_2$ are unit vectors in the illumination and observation directions respectively, and $\mathbf{d}$ is the displacement vector at the point of observation on the surface of the sample. When a relatively flat surface is intentionally oriented normal to the angle bisector of $\mathbf{e}_1$ and $\mathbf{e}_2$, the interferometer senses only the out-of-plane displacement component, W, and eqn (1) becomes

$$n\lambda = 2W \cos \beta \tag{2}$$

where 2β is the angle between the propagation vectors in the direction of illumination and observation. A carrier pattern can be superimposed on this deformation to allow the fringe pattern to be sufficiently simplified for digital recording. Equation (2) characterizes the deflection when the carrier pattern is recorded separately and numerically subtracted from the superimposed deformation.

The surfaces best suited to automated analysis are reasonably well behaved, relatively flat, and of nearly uniform reflectance. Unfortunately, in most real problems the surfaces of interest move in a very complex manner, have irregular surface contours, and exhibit non-uniform reflectance.

FEASIBILITY STUDIES

In prior related research, the basic functionality of an automated holographic recording and analysis system was demonstrated by its application to a study of the problem of a centrally loaded disk clamped around its boundary. Figure 1a shows a conventional holo-interferometric fringe pattern for an edge-clamped, centrally loaded disk, as well as the holo-interferometric fringe patterns obtained when the disk was rotated while in the unloaded state to produce a carrier fringe pattern (Fig. 1b) and then centrally loaded to produce a perturbed

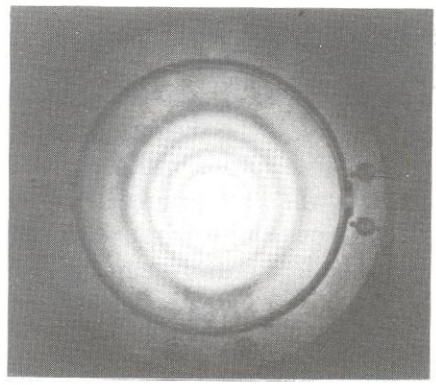

(a)

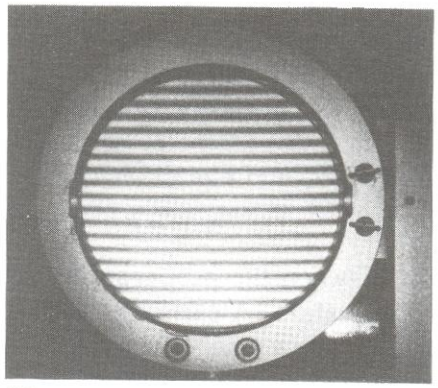

(b)

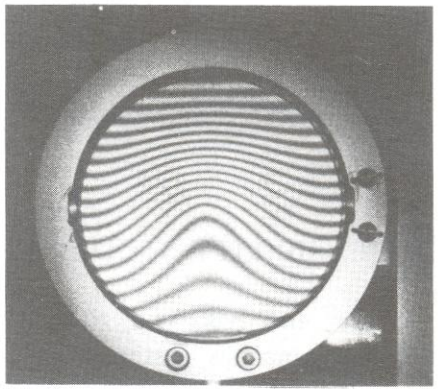

(c)

Fig. 1. (a) A holo-interferometric fringe pattern on the surface of a centrally loaded disk with no carrier fringes (no rotation). (b) A holo-interferometric carrier fringe pattern on the surface of an unloaded, undeformed disk subjected to a pure rotation. (c) A holo-interferometric fringe pattern on the surface of a centrally loaded disk. The fringes here are a combination of a carrier pattern produced by rotation and a deformation pattern due to the central loading.

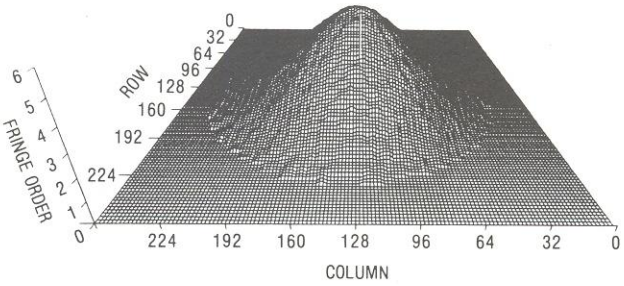

Fig. 2. A perspective plot of the deflection of the centrally loaded disk, obtained by fully automated analysis of the fringe patterns shown in Figs 1b and 1c.

or modulated carrier fringe pattern (Fig. 1c). Finally, Fig. 2 shows a plot of the surface deflection of the disk obtained by a completely automated processing of the holo-interferograms of Figs. 1b and 1c.[7] In this case, the edge of the specimen was fixed, which greatly simplified the identification of absolute fringe orders.

The next stage in developing this process was to apply it to a component with less constrained boundaries. A package used to house microelectronic circuit cards was used for this demonstration. This housing is made from two thin plastic shells sealed together along their edges, producing a hollow container about 9·0 cm long by 5·0 cm wide by 1·2 cm thick, suitable for holding an electronic circuit card. A photograph of the top surface of this housing is shown in Fig. 3a. It was aligned in the holo-interferometer shown in Fig. 4 so that the out-of-plane displacement could be measured (using eqn (2)) with a fringe sensitivity of 0·317 μm ($\beta = 4{\cdot}58°$). The illuminating and reference beams were guided through single mode optical fibers.

The housing was fitted with an air valve and rubber hose so that surface deformations could be produced by elevating the internal pressure, and then mounted on a rotation stage to allow generation of the carrier pattern. Using a thermoplastic holocamera a hologram was made of the package, and then the package was rotated 0·0114° about a horizontal axis so that the top of the package moved toward the observer. A photograph was then taken of the real-time fringe pattern caused by interference between the wavefront from the holographic image of the package and the wavefront from the actual package. The internal pressure of the package was elevated and another photograph of the real-time fringe distribution was taken. These photographs are shown in Figs 3b and 3c. A simple holo-interferogram of the same deformation field is shown in Fig. 3d for purposes of comparison.

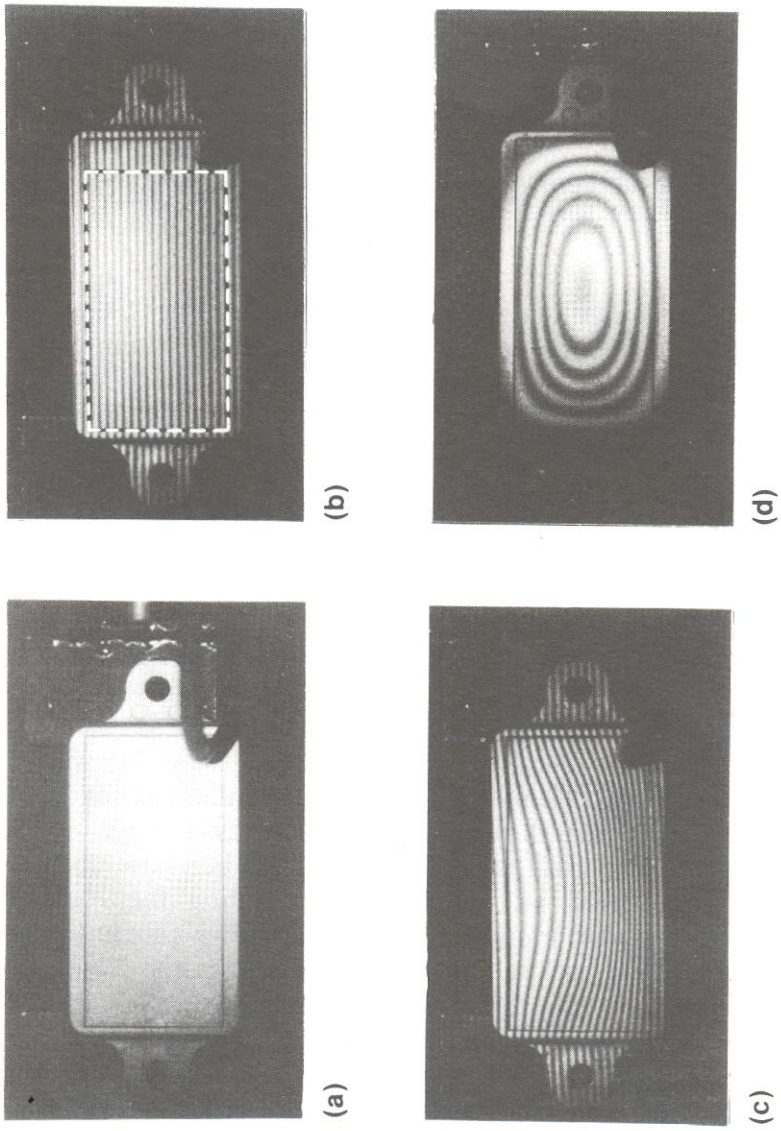

Fig. 3. (a) Photograph of the hermetically sealed housing used in the experiment. The dotted lines show the location of the area selected for analysis. (b) A holo-interferometric carrier fringe pattern produced by rotating the housing around a horizontal axis with the top moving toward the obsever. (c) The carrier fringe pattern shown in Fig. 3 modulated by the surface deflections caused by a change in internal pressure of the housing. (d) A deflection fringe pattern caused by a change in internal pressure. The housing was not rotated so there are no carrier fringes.

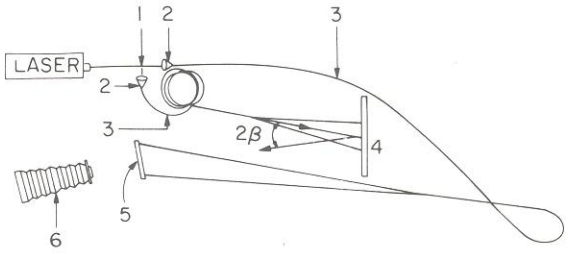

Fig. 4. A real-time holographic/fiber optic recording system. 1, variable beam splitter; 2, fiber launch optics; 3, single mode optical fiber; 4, model; 5, hologram plate; 6, camera system.

METHOD OF ANALYSIS

Since the direction of rotation of the housing is known, all the information needed to contour the deformed surface is contained in these two photographs. The contour analysis is begun by digitizing the holo-interferometric images shown in Figs 3b and 3c. The pictures were digitized using a vidicon camera with a resolution of 1024×1024 pixels and a grey scale range of 256 levels. It was decided to perform the analysis first along the vertical centerline of the surface, so for both photographs the intensity values of column 512 were selected out of the data arrays. Plots of these values are shown in Fig. 5. Various methods have been proposed for determining the phase change from such intensity plots. One common method is to transform to the Fourier domain and determine phase by analyzing the real and imaginary parts of each complex Fourier component.[5,10,11] In this paper, however, the Fourier analysis is used only to determine the carrier frequency and to remove noise from the signal. The phase is determined by curve fitting and interpolation techniques applied in the real domain. The details of the method follow.

The values from the undeformed image (Fig. 5a) were put through a fast Fourier transform to find the carrier frequency and all other frequencies were removed. The resulting data were then transformed back to the spatial domain using an inverse fast Fourier transform to obtain a smooth intensity distribution showing the basic carrier frequency. The data from the deformed image (Fig. 5b) were also transformed with a fast Fourier transform and the knowledge of the carrier frequency obtained from the undeformed image was used to set a bandpass filter to remove noise from the data. The filtered data were then transformed back to the spatial domain as a smooth intensity distribution showing the combined results of the carrier and deforma-

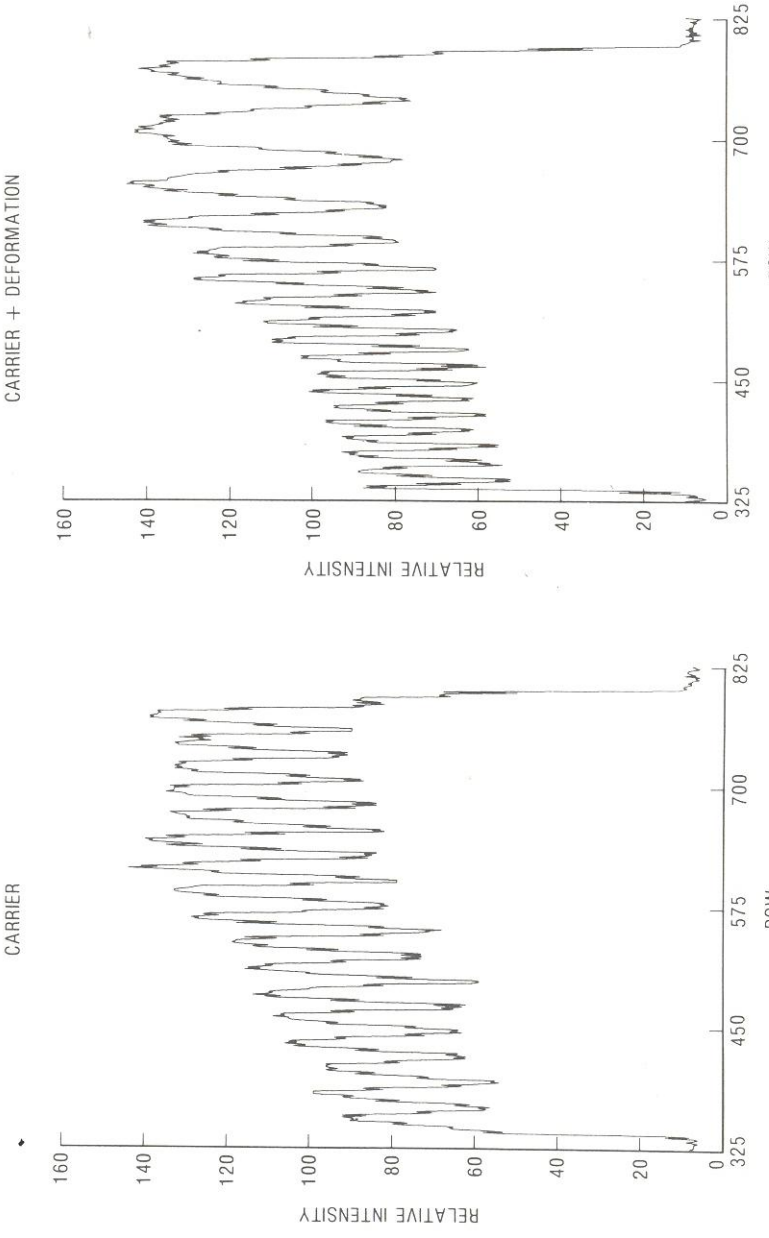

Fig. 5. (a) Intensity distribution for column 512 from data array of housing with carrier fringes only. (b) Intensity distribution for column 512 from data array of housing with fringes due to both carrier and deformation

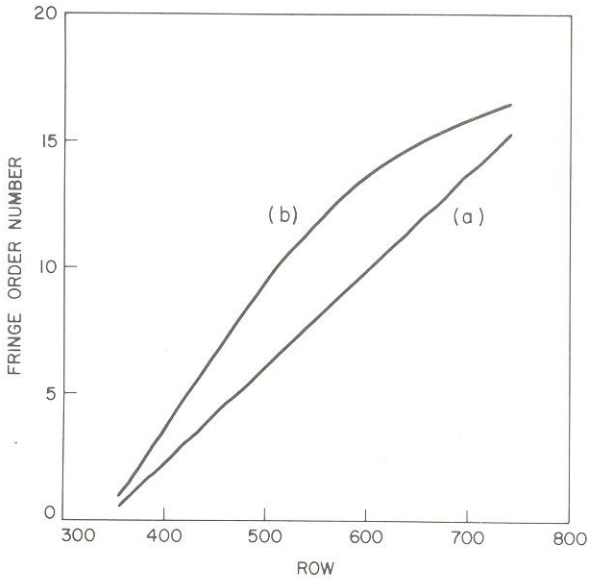

Fig. 6. Fringe order plots of (a) the carrier, and (b) the carrier plus deformation, along the vertical centerline of the hermetically sealed housing (column 512).

tion fringe patterns. In order to determine the fringe orders, the computer next proceeded to locate the extrema of the intensity distributions for each filtered fringe pattern. This was done by applying standard methods of data analysis[12] to fit curves through the data points, and then differentiating to locate the desired extrema. Figure 6 shows fringe order versus row number plots along the vertical centerline for both the unloaded and the loaded housing. Curve 'a' is for the unloaded housing (carrier only) while curve 'b' is for the loaded housing (carrier plus deformation). The linear curve 'a' obtained for the unloaded case is simply a manifestation of the simple sinusoidal pattern of fringes across the face of the housing. In curve 'b', for the loaded condition, there is a rapid phase change across the lower part of the housing where the intensity fringes were crowded together, and then a slow phase change across the upper part where the fringes were spaced out.

Since curve 'a' of Fig. 6 gives information concerning the phase change due to the carrier while curve 'b' of the same figure gives the corresponding information for the carrier plus deformation, the next step in the process was to subtract the two curves. A cubic spline technique[13] was used to interpolate values for each row of the two curves, and these values were then subtracted from each other to get

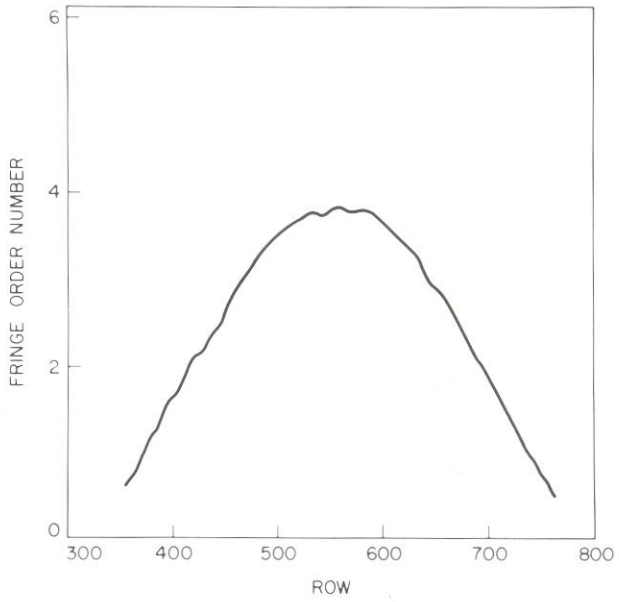

Fig. 7. Fringe order plot corresponding to the deflection along the vertical centerline of the housing (column 512).

the distribution of phase change due to the deformation alone. This result is shown in Fig. 7, which is a plot of the out-of-plane deformation of the surface across the vertical centerline from the bottom to the top of the housing as oriented in Fig. 3.

WINDOWING

An attempt to apply the above process to obtain the deflection across the entire specimen immediately showed a major limitation of the automated fringe analysis. The main problem was that surface ridges near the boundaries of the specimen introduced very rapid fluctuations in the fringes which prevented the automated system from performing valid analysis. In order to simplify the analysis and solve this problem, a method of windowing the data field was developed. This method has a number of advantages. First, it allows the user to select a subregion of interest from a larger array of data. If desired, this subregion can be magnified by zooming in on the desired region as described below. Also, the process permits the analysis of a multilevel surface where ridges and/or shadows cause discontinuities in the holo-interferometric fringe pattern. Finally, the windowing technique can be used to

effectively eliminate regions of the digitized data that may cause difficulty or be incorrectly interpreted by the scanning algorithm.

If no magnification of the subregion is desired, one can easily create a window in the original array of digitized data by simply resetting all rows and columns outside the desired region to zero. A short program was written which allowed the determination of the boundaries of the window from a video display of the digitized image. Of course, the same window must be used on both the carrier and carrier plus deformation data arrays. The window chosen here is indicated by the dotted lines in Fig. 3b, where the top, bottom and left borders were chosen to eliminate surface ridges from the area to be analyzed. The vertical border on the right was selected to eliminate the air valve with its rubber hose from the region to be analyzed. Note that the asymmetry in the final plot shown in Fig. 9a is due to the fact that the left edge of the plot corresponds to an area of the housing near one of its sealed edges, whereas the right edge of the plot represents an area of the housing closer to the center of the unit. The deformation near the center is of course considerably greater than the deformation near the edge. This is also clearly shown in Fig. 8, where the four graphs represent the surface deflection at different columns spaced across the housing surface. Very little deflection is observed in column 48, near a sealed edge, while a large deflection is found at column 512, which is

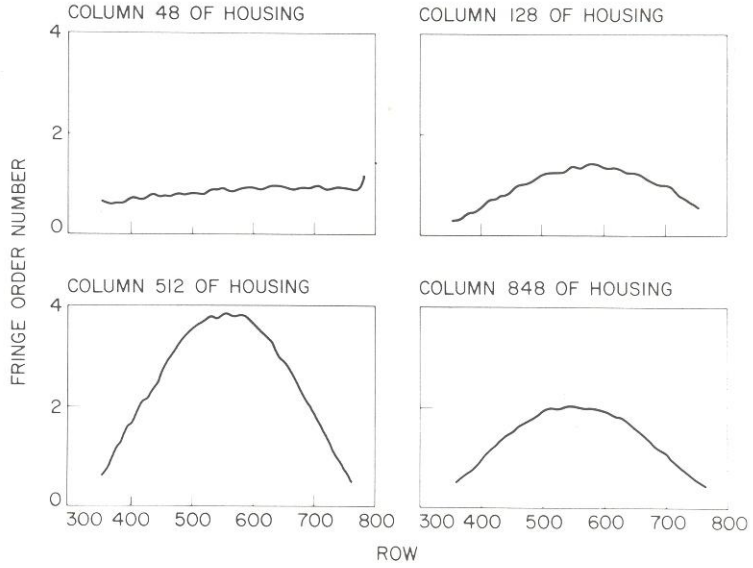

Fig. 8. Graphs of the surface deflection at various columns across the surface of the housing.

approximately the middle of the surface. Column 848 shows that the deflection is decreasing as the right window boundary is approached.

If it is desired to obtain a magnified image of a subregion, the camera can be zoomed in on the selected region, and the window borders can be specified later by mathematically resetting to zero all rows and columns outside the desired area.

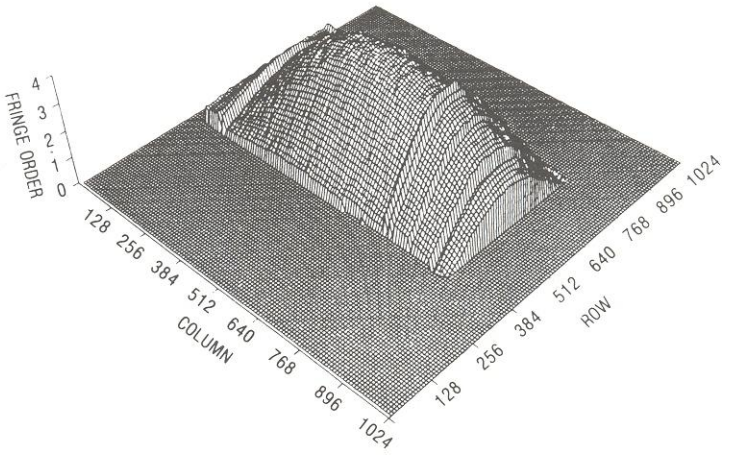

(a)

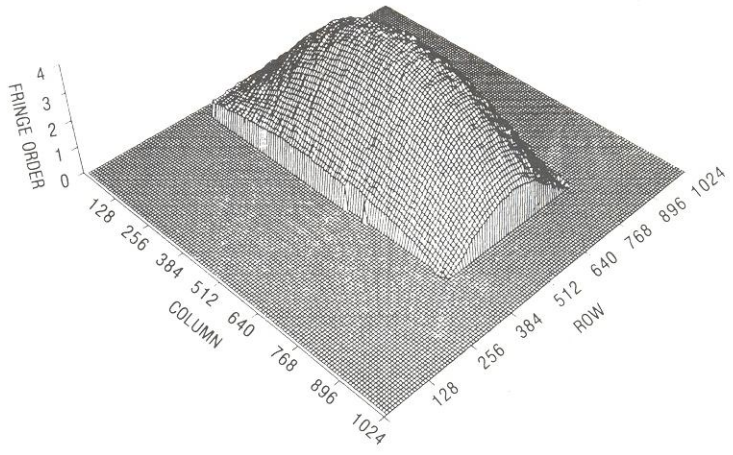

(b)

Fig. 9. (a) Plot of the surface deflection of the housing for the subregion outlined with dashed lines in Fig. 3b. The irregularities in the surface are due to errors in fringe counting. (b) Plot of the surface deflection of the housing for the subregion outlined with dashed lines in Fig. 3b. To obtain this plot, an improved fringe counting algorithm was used which monitored the gain or loss of fringes at the bottom boundary.

FRINGE COUNTING

A second problem arose because of difficulties in automatically assigning fringe orders. The successful use of the windowing technique depends on the development of an algorithm which can properly compensate for the gain or loss of a fringe along the window boundary where scanning begins. Sudden changes in the fringe count due to the gain or loss of a fringe resulted in discontinuities in the final plot. An example of such a faulty plot is shown in Fig. 9a. The solution to this problem is to make use of the nearly linear (slowly varying) character of the fringe field. Discontinuities in the deformation field between the first fringe and the window boundary are taken to signal the gain or loss of a fringe and an appropriate adjustment to the fringe count is made automatically. Fig 9b shows a plot of results from the same data used in Fig. 9a, as analyzed with a modified program containing the improved fringe count compensating algorithm.

CONCLUSION

A method for automating the measurement of complex deformations has been developed. In earlier work involving a centrally loaded disk with a clamped boundary, excellent results were easily obtained, since the disk had fixed boundary conditions and a flat surface with relatively uniform reflectivity. However, in the case of the sealed housing experiment described in this paper, problems due to surface irregularities and fringe discontinuities at the edges of the specimen posed problems. These were overcome by the use of a windowing technique together with an improved fringe counting algorithm. The basic reason that these successful results were obtained from a very simple technique was the introduction of the carrier which produced a smooth monotonic phase variation creating nearly straight fringes with a large number of data points per fringe. This allowed simple curve fitting routines to be used in determining the location of the fringes and thus determine the phase at each point. On the other hand, the Fourier transform techniques alluded to earlier do not require any curve fitting but introduce the need for 'phase-unwrapping'[10] procedures. Both techniques face the same problem in establishing a proper fringe count at the boundaries.

ACKNOWLEDGEMENTS

The authors wish to acknowledge the support of AT&T Bell Laboratories, Murray Hill, NJ, Marquette University, and the University of

Alabama in Huntsville. Since 1980, Professor Gilbert's efforts in holography have been supported in part by contracts DAAG 29-84-K-0183, DAAG 29-84-G-0045 and DAAL 03-86-K-0014 with the Army Research Office in Research Triangle Park, NC.

REFERENCES

1. F. Lanzl and M. Schulter, Microprocessor-controlled hologram analysis, *IEEE 5th International Computing Conference*, London, 1978, pp. 159–62.
2. J. P. Hot and C. Durou, System for the automatic analysis of interferograms obtained by holographic interferometry, *SPIE 2nd European Congress on Optics Applied to Metrology* **210**, 1979, pp. 144–51.
3. F. Lamy, C. Liegeois and P. Meyrueis, Automatic computer analysis of double exposure holograms in industrial nondestructive control, *Proc. SPIE*, **353** (1983) 82–9.
4. Y. Katzir, A. A. Friesem, I. Glaser and B. Sharon, Holographic nondestructive evaluation with on-line acquisition and processing, *Industrial and Commercial Applications of Holography*, Milton Chang (ed.), *Proc. SPIE*, **353** (1982) 74–81.
5. C. A. Sciammarella and M. Ahmadshahi, Computer based method for fringe pattern analysis, *Proc. of the* 1984 *SEM Fall Conference,* Milwaukee, WI, 1984, pp. 61–9.
6. P. D. Plotkowski, Y. Y. Hung, J. D. Hovanesian and G. Gerhart, Improved fringe carrier technique for unambiguous determination of holographically recorded displacements, *Opt. Engng*, **24** (1985) 754–6.
7. D. R. Matthys, T. D. Dudderar and J. A. Gilbert, Automated analysis of holo-interferograms for determination of surface displacements, *Exp. Mech.* (in press).
8. J. A. Gilbert, T. D. Dudderar, M. E. Schultz and A. J. Boehnlein, The monomode fiber—a new tool for holographic interferometry, *Exp. Mech.*, **23** (1983) 190–5.
9. T. D. Dudderar and J. A. Gilbert, Real-time holographic interferometry through fiber optics, *J. Phys. E: Sci. Instrum.*, **18** (1985) 39–43.
10. M. T. Takeda, H. Ina and S. Kobayashi, Fourier-transform method of fringe-pattern analysis for computer-based topography and interferometry, *J. Opt. Soc. Am.*, **72** (1) (1982) 156–60.
11. T. Kreis, Digital holographic interference-phase measurement using the Fourier-transform method. *J. Opt. Soc. Am. A,* **3** (1986) 847–53.
12. A. Savitzky and J. E. Golay, Smoothing and differentiation of data by simplified least squares, *Analyt. Chem.*, **36** (1964) 1627–39.
13. H. Akima, New method of interpolation and smooth curve fitting based on local procedures, *J. ACM* **17**(4) (1970) 589–602.